Appl. Math. Mech. -Engl. Ed., **33**(8), 1001–1014 (2012)
DOI 10.1007/s10483-012-1601-9

Applied Mathematics and Mechanics (English Edition)

Effect of viscous dissipation and heat source on flow and heat transfer of dusty fluid over unsteady stretching sheet*

B. J. GIREESHA, G. S. ROOPA, C. S. BAGEWADI

(Department of Studies and Research in Mathematics, Kuvempu University, Shankaraghatta 577451, Karnataka, India)

Abstract This paper investigates the problem of hydrodynamic boundary layer flow and heat transfer of a dusty fluid over an unsteady stretching surface. The study considers the effects of frictional heating (viscous dissipation) and internal heat generation or absorption. The basic equations governing the flow and heat transfer are reduced to a set of non-linear ordinary differential equations by applying suitable similarity transformations. The transformed equations are numerically solved by the Runge-Kutta-Fehlberg-45 order method. An analysis is carried out for two different cases of heating processes, namely, variable wall temperature (VWT) and variable heat flux (VHF). The effects of various physical parameters such as the magnetic parameter, the fluid-particle interaction parameter, the unsteady parameter, the Prandtl number, the Eckert number, the number density of dust particles, and the heat source/sink parameter on velocity and temperature profiles are shown in several plots. The effects of the wall temperature gradient function and the wall temperature function are tabulated and discussed.

Key words heat transfer, boundary layer flow, stretching surface, dusty fluid, viscous dissipation, non-uniform heat source, numerical solution

Chinese Library Classification O359$^+$.1, O414.1
2010 Mathematics Subject Classification 76T15, 80A20

1 Introduction

In recent years, a great deal of interest has been generated in the area of boundary layer flow and heat transfer of a fluid over a stretching sheet. In view of its numerous and wide range of applications in various fields such as polymer processing industry in particular manufacturing process of artificial films, artificial fibers, and dilute polymer solutions. To be more specific, it may be pointed out that many metallurgical processes involve the cooling of continuous strips or filaments by drawing them through a quiescent fluid, and in the process of drawing, these strips are sometimes stretched. The heat transfer analysis over a stretching surface is of much practical interest due to its abundant applications such as heat-treated materials travelling between a feed roll and wind-up roll or materials manufactured by extrusion, glass-fiber, and paper production, cooling of metallic sheets or electronic chips, drawing of plastic films, liquid

* Received Apr. 2, 2011 / Revised Mar. 28, 2012
Project supported by the Major Research Project of Department of Science and Technology (DST) of New Delhi (No. SR/S4/MS:470/07, 25-08-2008)
Corresponding author B. J. GIREESHA, Ph. D., E-mail: bjgireesu@rediffmail.com

films in condensation processes. Due to the high applicability of this problem in the industrial phenomena, it has attracted attention of many researchers.

Sakiadis[1–2] studied the boundary layer problem by assuming the velocity of a boundary sheet as a constant. The two-dimensional steady flow of an incompressible viscous fluid caused by a linearly stretching plate was discussed by Crane[3]. The temperature field in the flow of a fluid over a linearly stretching surface subject to a uniform unit flux was studied by Grubka and Bobba[4]. The effects of the buoyancy force on the development of the velocity and thermal boundary layer flows over a stretching sheet were first studied by Chen[5]. Elbashbeshy and Bazid[6], Sharidan et al.[7], and Tsai et al.[8] obtained a similarity solution for the flow and heat transfer of a fluid over an unsteady stretching surface. The problem of mixed convection adjacent to a vertical continuously stretching sheet in the presence of a variable magnetic field was studied by Ishak et al.[9]. Aziz[10] obtained the numerical solution for the laminar thermal boundary over a flat plate with a convective surface boundary condition using the symbolic algebra software MAPLE. Vajravelu and Roper[11] studied the flow and heat transfer in a second grade fluid over a stretching sheet.

The effect of viscous dissipation changes the temperature distributions by playing a role as an energy source, which affects the heat transfer rates. The merit of the effect of viscous dissipation depends on whether the plate is being cooled or heated. Chen[12] examined the effect of combined heat and mass transfer on magnetohydrodynamic (MHD) free convection from a vertical surface with the Ohmic heating and viscous dissipation. Pal and Hiremath[13] determined the heat transfer characteristics in the laminar boundary layer flow over an unsteady stretching sheet placed in a porous medium in the presence of viscous dissipation and internal absorption or generation. The analytical results were carried out by Vajravelu and Hadjinicolaou[14] who took the effects of viscous dissipation and internal heat generation into account. Veena et al.[15] obtained the solutions of heat transfer in a visco-elastic fluid past a stretching sheet with viscous dissipation and internal heat generation.

In light of the above investigations, it is found that these studies are restricted to the fluid flow and heat transfer problems. However, the fluid flow embedded with dust particles is encountered in different engineering problems concerned with nuclear reactor cooling, powder technology, rain erosion, paint spraying, etc. The important applications of dust particles in the boundary layer include soil erosion by natural winds and dust entrainment in a cloud during a nuclear explosion. It also occurs in a wide range of technical processes like fluidization, flow in rocket tubes, combustion, and purification of crude oil. In view of these applications, Saffman[16] discussed the stability of the laminar flow of a dusty gas, in which the dust particles were uniformly distributed. Datta and Mishra[17] investigated the boundary layer flow of a dusty fluid over a semi-infinite flat plate by considering the drag force due to slip and the transverse force due to slip-shear in the boundary layer equations. Agranat[18] discussed the combined effects of the dustiness and the pressure gradient on the friction and heat transfer coefficients. These results are used for the practical calculation of the friction and heat transfer in a quasi-equilibrium dusty laminar boundary layer and also used for interpreting the corresponding experimental data.

Vajravelu and Nayfeh[19] discussed the analysis of hydromagnetic flow of a dusty fluid over a stretching sheet including the effects of suction. Xie et al.[20] addressed the stability equation for the particle-laden Blasius flow using the Saffmans formulation. Palani and Ganesan[21] investigated the flow of dusty gas past a semi-infinite isothermal inclined plate. Recently, Gireesha et al.[22] studied the steady boundary layer flow and heat transfer of a dusty fluid over a stretching sheet taking non-uniform heat source/sink into account. In this analysis, they studied two types of heating processes, namely, the prescribed surface temperature (PST) and the prescribed heat flux (PHF) cases in the absence of the magnetic field and viscous dissipation effect. Furthermore, they analyzed the effects of the fluid particle interaction parameter, the Eckert number, the Prandtl number, the number density of the dust particle, and the non-uniform heat generation/absorption parameter on temperature distributions.

Now, we extend the work of Gireesha et al.[22] for unsteady flow by taking the combined effects of the viscous dissipation and the magnetic field on heat transfer into account, which is important in view point of desired properties of the outcome. Here, we examine the thermal problem for two cases of boundary heating, i.e., the variable wall temperature (VWT) and the variable heat flux (VHF). Highly non-linear momentum and heat transfer equations are numerically solved using the Runge-Kutta-Fehlberg-45 order method with the software MAPLE. Furthermore, the effects of different flow parameters like the magnetic parameter, the fluid particle interaction parameter, the unsteady parameter, the Eckert number, the Prandtl number, the number density of the dust particle, and the heat source/sink parameter on velocity profiles and temperature distributions are discussed. The skin friction coefficient and the local Nusselt number are also discussed in detail.

2 Mathematical formulation and solution to problem

Consider the unsteady two-dimensional laminar boundary layer flow and heat transfer of an incompressible viscous dusty fluid over a stretching sheet. The x-axis is taken along the stretching surface in the direction of the motion with the slot as the origin, and the y-axis is perpendicular to the sheet in the outward direction towards the fluid. The flow is assumed to be confined in a region of $y > 0$. The flow is caused by the stretching of the sheet which moves in its own plane with the surface velocity $U_{\rm w}(x,t)$. It is considered that the wall temperature $T_{\rm w}(x,t)$ of the sheet is suddenly raised from T_∞ to $T_{\rm w}(x,t)\,(T_{\rm w}(x,t) > T_\infty)$, or there is a suddenly imposed heat flux $q_{\rm w}(x,t)$ at the wall. In order to obtain the effect of temperature difference between the surface and the ambient fluid, we consider the temperature-dependent heat source/sink in the flow. The frictional heating due to viscous dissipation is also taken into account. Under these situations, the governing two-dimensional boundary layer equations for momentum take the following forms[19]:

$$\frac{\partial u}{\partial x}+\frac{\partial u}{\partial y}=0, \tag{1}$$

$$\frac{\partial u}{\partial t}+u\frac{\partial u}{\partial x}+v\frac{\partial u}{\partial y}=\frac{\mu}{\rho}\frac{\partial^2 u}{\partial y^2}+\frac{KN}{\rho}(u_{\rm p}-u)-\frac{\sigma\widehat{B}_0^2}{\rho}u, \tag{2}$$

$$\frac{\partial u_{\rm p}}{\partial t}+u_{\rm p}\frac{\partial u_{\rm p}}{\partial x}+v_{\rm p}\frac{\partial u_{\rm p}}{\partial y}=\frac{K}{m}(u-u_{\rm p}), \tag{3}$$

$$\frac{\partial v_{\rm p}}{\partial t}+u_{\rm p}\frac{\partial v_{\rm p}}{\partial x}+v_{\rm p}\frac{\partial v_{\rm p}}{\partial y}=\frac{K}{m}(v-v_{\rm p}), \tag{4}$$

$$\frac{\partial(\rho_{\rm p}u_{\rm p})}{\partial x}+\frac{\partial(\rho_{\rm p}v_{\rm p})}{\partial y}=0, \tag{5}$$

where x and y represent the coordinate axes along the continuous surface in the direction of motion and perpendicular to it, respectively, (u,v) and $(u_{\rm p},v_{\rm p})$ denote the velocity components of the fluid and the particle phase along the x- and y-directions, respectively, t is the time, μ is the coefficient of viscosity of fluid, ρ and $\rho_{\rm p}$ are the densities of the fluid and the particle phase, respectively, $\widehat{B}_0$ is the induced magnetic field, N is the number density of the particle phase, K is Stoke's resistance coefficient, σ is the electrical conductivity, and m is the mass concentration of dust particles. In deriving these equations, the Stokesian drag force is considered for the interaction between the fluid and the particle phase, and the induced magnetic field is neglected. Also, it is assumed that the external electric field is zero, and the electric field as a result of polarization of charges is negligible.

The associate boundary conditions for the above boundary layer equations are considered as

$$\begin{cases} u=U_{\rm w}(x,t), \quad v=V_{\rm w}(x,t) \quad \text{at} \quad y=0, \\ u\to 0, \quad u_{\rm p}\to 0, \quad v_{\rm p}\to 0, \quad \rho_{\rm p}\to E\rho \quad \text{as} \quad y\to\infty, \end{cases} \tag{6}$$

where $U_{\mathrm{w}}(x,t) = \frac{bx}{1-at}$ is the sheet velocity, and a (the stretching rate) and b are positive constants with dimension t^{-1}. It is noted that the stretching rate $\frac{b}{1-at}$ increases with time since $a > 0$. In the context of polymer extrusion, the material properties and in particular the elasticity of the extruded sheet may vary with time even though the sheet is being pulled by a constant force. With the unsteady stretching (i.e., $a \neq 0$), however, a^{-1} becomes the representative time scale of the resulting unsteady boundary layer problem. $V_{\mathrm{w}}(x,t) = -\frac{v_0}{\sqrt{(1-at)}}$ is the velocity of suction ($V_{\mathrm{w}}(x,t) > 0$), and E is the density ratio.

The mathematical complexity of the problem is simplified by introducing the following dimensionless coordinates in terms of the similarity variable η and the similarity function f:

$$\begin{cases} u = \dfrac{bx}{1-at} f'(\eta), \quad v = -\sqrt{\dfrac{b\nu}{1-at}} f(\eta), \quad \eta = \sqrt{\dfrac{b}{\nu(1-at)}} y, \\ u_{\mathrm{p}} = \dfrac{bx}{1-at} F(\eta), \quad v_{\mathrm{p}} = \sqrt{\dfrac{b\nu}{1-at}} G(\eta), \quad \rho_{\mathrm{r}} = H(\eta), \quad \widehat{B}_0 = B_0(1-at)^{-\frac{1}{2}}, \end{cases} \tag{7}$$

where a prime denotes the differentiation with respect to η, and $\rho_{\mathrm{r}} = \frac{\rho_{\mathrm{p}}}{\rho}$ is the relative density.

Substituting (7) into the governing equations (1)–(5), we obtain

$$f'''(\eta) + f(\eta) f''(\eta) - f'(\eta)^2 - \alpha\Big(f'(\eta) + \frac{\eta}{2} f''(\eta)\Big) + l\beta H(\eta)(F(\eta) - f'(\eta)) - M f'(\eta) = 0, \tag{8}$$

$$G(\eta)F'(\eta) + F(\eta)^2 - \beta(f'(\eta) - F(\eta)) + \alpha\Big(F(\eta) + \frac{\eta}{2} F'(\eta)\Big) = 0, \tag{9}$$

$$G(\eta)G'(\eta) + \beta(f(\eta) + G(\eta)) + \frac{\alpha}{2}(G(\eta) + \eta G'(\eta)) = 0, \tag{10}$$

$$F(\eta)H(\eta) + G'(\eta)H(\eta) + H'(\eta)G(\eta) = 0, \tag{11}$$

and the boundary conditions become

$$\begin{cases} f'(\eta) = 1, \quad f(\eta) = f_0 \quad \text{at} \quad \eta = 0, \\ f'(\eta) = 0, \quad F(\eta) = 0, \quad G(\eta) = -f(\eta), \quad H(\eta) = E \quad \text{as} \quad \eta \to \infty, \end{cases} \tag{12}$$

where $\alpha = \frac{a}{b}$ is a parameter that measures the unsteadiness, $M = \frac{\sigma B_0^2}{\rho b}$ is the magnetic parameter, $l = \frac{mN}{\rho_{\mathrm{p}}}$ is the mass concentration, $\beta = \frac{1}{\tau_{\mathrm{v}} b}(1-at)$ is the local fluid-particle interaction parameter, $\tau_{\mathrm{v}} = \frac{m}{K}$ is the relaxation time of the particle phase, and $f_0 = \frac{v_0}{\sqrt{b\nu}}$ ($f_0 > 0$) is the suction parameter.

3 Heat transfer analysis

The governing unsteady dusty boundary layer heat transport equations with the thermal conductivity, viscous dissipation, and non-uniform heat source are given by[23]

$$\rho c_p\Big(\frac{\partial T}{\partial t} + u\frac{\partial T}{\partial x} + v\frac{\partial T}{\partial y}\Big) = k\frac{\partial^2 T}{\partial y^2} + \frac{N c_p}{\tau_{\mathrm{T}}}(T_{\mathrm{p}} - T) + \frac{N}{\tau_{\mathrm{v}}}(u_{\mathrm{p}} - u)^2 + \mu\Big(\frac{\partial u}{\partial y}\Big)^2 + Q(T - T_\infty), \tag{13}$$

$$N c_{\mathrm{m}}\Big(\frac{\partial T_{\mathrm{p}}}{\partial t} + u_{\mathrm{p}}\frac{\partial T_{\mathrm{p}}}{\partial x} + v_{\mathrm{p}}\frac{\partial T_{\mathrm{p}}}{\partial y}\Big) = -\frac{N c_p}{\tau_{\mathrm{T}}}(T_{\mathrm{p}} - T), \tag{14}$$

where T and $T_{\rm p}$ are the temperatures of the fluid and the dust particle inside the boundary layer, respectively, c_p and $c_{\rm m}$ are the specific heat of the fluid and the dust particles, respectively, $\tau_{\rm T}$ is the thermal equilibrium time and is the time required by a dust cloud to adjust its temperature to the fluid, k is the thermal conductivity, and the term Q represents the heat source when $Q>0$ and the sink when $Q<0$.

To solve the temperature equations (13) and (14), consider two general cases of temperature boundary conditions, namely, VWT and VHT.

Case 1 VWT

For this heating process, the following variable wall temperature boundary conditions are used:

$$\begin{cases} T = T_{\rm w}(x,t) \quad \text{at} \quad y=0, \\ \\ T \to T_\infty, \quad T_{\rm p} \to T_\infty \quad \text{as} \quad y \to \infty, \end{cases} \tag{15}$$

where $T_{\rm w} = T_\infty + T_0\big(\frac{bx^2}{\nu(1-at)^2}\big)$ is the surface temperature of the sheet varing with the distance x from the slot and the time t, T_0 is a reference temperature such that $0 \leqslant T_0 \leqslant T_{\rm w}$, and T_∞ is the temperature far away from the stretching surface with $T_{\rm w} > T_\infty$. The expression $T_{\rm w}$ reflects that the sheet temperature decreases from T_0 at the slot in proportion to x^2, and the temperature reduction increases with an increase in $(1-at)$. However, it should be noticed that equations of $U_{\rm w}$ and $T_{\rm w}$, which are responsible for the whole analysis, are valid only for $t < \frac{1}{a}$.

Introduce the dimensionless variables for the temperatures $\theta(\eta)$ and $\theta_{\rm p}(\eta)$ as follows:

$$\theta(\eta) = \frac{T-T_\infty}{T_{\rm w}-T_\infty}, \quad \theta_{\rm p}(\eta) = \frac{T_{\rm p}-T_\infty}{T_{\rm w}-T_\infty}, \tag{16}$$

where $T - T_\infty = T_0\big(\frac{bx^2}{\nu(1-at)^2}\big)\theta(\eta)$.

Using the similarity variable η and (16) into (13) and (14), we can obtain the following dimensionless system of equations:

$$\theta''(\eta) + Pr(f(\eta)\theta'(\eta) - 2f'(\eta)\theta(\eta)) + \frac{N}{\rho}c_1 Pr(\theta_{\rm p}(\eta) - \theta(\eta)) + Pr\delta\theta(\eta)$$

$$+ \frac{N}{\rho}\beta PrEc(F(\eta) - f'(\eta))^2 - \frac{\alpha}{2}Pr(4\theta(\eta) + \eta\theta'(\eta)) + PrEc(f''(\eta))^2 = 0, \tag{17}$$

$$G(\eta)\theta'_{\rm p}(\eta) + 2F(\eta)\theta_{\rm p}(\eta) + \frac{\alpha}{2}(4\theta_{\rm p}(\eta) + \eta\theta'_{\rm p}(\eta)) + c_1\gamma(\theta_{\rm p}(\eta) - \theta(\eta)) = 0, \tag{18}$$

where $Pr = \frac{\mu c_p}{k}$ is the Prandtl number, $c_1 = \frac{1}{\tau_{\rm T} b}(1-at)$ is the local fluid-particle interaction parameter for temperature, $\delta = \frac{Qk}{\mu c_p}\frac{Re_x}{Re_k^2}$ is the source sink parameter, $\gamma = \frac{c_p}{c_{\rm m}}$ is the ratio of c_p and $c_{\rm m}$, $Ec = \frac{{U_{\rm w}}^2}{c_p(T_{\rm w}-T_\infty)}$ is the local Eckert number, $Re_x = \frac{U_{\rm w}x}{\nu}$ is the local Reynolds number, and $Re_k = \frac{U_{\rm w}\sqrt{k}}{\nu}$.

The corresponding thermal boundary conditions are given by

$$\begin{cases} \theta(\eta) = 1 \quad \text{at} \quad \eta = 0, \\ \\ \theta(\eta) \to 0, \quad \theta_{\rm p}(\eta) \to 0 \quad \text{as} \quad \eta \to \infty. \end{cases} \tag{19}$$

Case 2 VHF

In the VHF case, define the boundary conditions of temperature as follows:

$$\begin{cases} \dfrac{\partial T}{\partial y} = -\dfrac{q_{\rm w}(x,t)}{k} & \text{at} \quad y = 0, \\ T \to T_\infty, \quad T_{\rm p} \to T_\infty & \text{as} \quad y \to \infty, \end{cases}$$

where $q_{\rm w}(x,t) = q_{\rm w_0} x^2 \left(\frac{b}{\nu}\right)^{3/2} (1-at)^{-5/2}$.

In order to obtain the similarity solution for temperature, define dimensionless temperature variables in the VHF case as follows:

$$g(\eta) = \frac{T - T_\infty}{T_{\rm w} - T_\infty}, \quad g_{\rm p}(\eta) = \frac{T_{\rm p} - T_\infty}{T_{\rm w} - T_\infty},$$

where $T = T_\infty + \frac{q_{\rm w_0}}{k}\left(\frac{bx^2}{\nu(1-at)^2}\right) g(\eta)$.

With (13) and (14), we can get the following equations in the non-dimensional forms:

$$g''(\eta) + Pr(f(\eta)g'(\eta) - 2f'(\eta)g(\eta)) + \frac{N}{\rho} c_1 Pr(g_{\rm p}(\eta) - g(\eta)) + Pr\delta g(\eta)$$

$$+ \frac{N}{\rho}\beta PrEc(F(\eta) - f'(\eta))^2 - \frac{\alpha}{2} Pr(4g(\eta) + \eta g'(\eta)) + PrEc(f''(\eta))^2 = 0, \tag{20}$$

$$G(\eta) g_{\rm p}'(\eta) + 2F(\eta) g_{\rm p}(\eta) + \frac{\alpha}{2}(4g_{\rm p}(\eta) + \eta g_{\rm p}'(\eta)) + c_1\gamma(g_{\rm p}(\eta) - g(\eta)) = 0. \tag{21}$$

The corresponding boundary conditions become

$$\begin{cases} g'(\eta) = -1 & \text{at} \quad \eta = 0, \\ g(\eta) = 0, \quad g_{\rm p}(\eta) = 0 & \text{as} \quad \eta \to \infty. \end{cases} \tag{22}$$

The physical quantities of interest are the skin friction coefficient $C_{\rm f}$ and the local Nusselt number Nu_x, which are, respectively, defined as

$$C_{\rm f} = \frac{\tau_{\rm w}}{\rho {U_{\rm w}}^2}, \quad Nu_x = \frac{x q_{\rm w}}{k(T_{\rm w} - T_\infty)}, \tag{23}$$

where the skin friction $\tau_{\rm w}$ and the heat transfer from the sheet $q_{\rm w}$ are, respectively, given by

$$\tau_{\rm w} = \mu\Big(\frac{\partial u}{\partial y}\Big)_{y=0}, \quad q_{\rm w} = -k\Big(\frac{\partial T}{\partial y}\Big)_{y=0}. \tag{24}$$

Using the non-dimensional variables, we obtain

$$C_{\rm f} {Re_x}^{1/2} = f''(0), \quad \frac{Nu_x}{{Re_x}^{1/2}} = -\theta'(0) \quad \text{(the VWT case)}, \quad \frac{Nu_x}{{Re_x}^{1/2}} = \frac{1}{g(0)} \quad \text{(the VHF case)}.$$

4 Numerical solution

Equations (8) and (11) together with the boundary conditions (12) form highly non-linear ordinary differential equations. In order to solve these equations numerically, we follow the most efficient numerical technique with the Runge-Kutta-Fehlberg-45 scheme with the software MAPLE. In this method, it is most important to choose an appropriate finite value of $\eta \to \infty$ (here, we take $\eta = 11$). The coupled boundary value problem equations (8)–(11) and either (17) and (18) (the VWT case) or (21) and (22) (the VHF case) are solved by the Runge-Kutta-Fehlberg-45 order method. The accuracy of the present numerical method is checked in comparison with the results obtained by Chen[5] and Ishak et al.[9] for the local Nusselt number in the limiting condition ($\alpha = \beta = M = N = Ec = 0$). Thus, it is seen from Table 1 that the numerical results are in close agreement with those published previously.

Table 1 Comparison of local Nusselt number Nu_x for several values of Pr with $\beta = \alpha = M = Ec = f_0 = \delta = 0$

Pr	Chen[5]	Ishak et al.[9]	Present study
0.72	1.088 5	–	1.088 5
1.00	1.333 3	1.333 3	1.333 3
3.00	2.509 7	2.509 7	2.509 7
10.0	4.796 8	4.796 9	4.796 8

5 Results and discussion

The hydromagnetic boundary layer flow and heat transfer of a dusty fluid over a stretching sheet can be investigated in the presence of viscous dissipation and non-uniform heat source/sink. Similarity transformations are used to convert the governing time-dependent non-linear boundary layer equations into a system of non-linear ordinary differential equations. The obtained highly non-linear ordinary differential equations are numerically solved. The temperature profiles for $\theta(\eta)$ and $\theta_{\mathrm{p}}(\eta)$ in the VWT case and $g(\eta)$ and $g_{\mathrm{p}}(\eta)$ in the VHF case are graphically depicted in the presence of internal heat generation/absorption. In order to have physical point of view of the problem, numerical calculations are carried out for different values of the magnetic parameter (M), the number density (N), the dust interaction parameter (β), the Prandtl number (Pr), the Eckert number (Ec), the heat source/sink parameter (δ), and the unsteadiness parameter (α). The comparison of the present results of heat transfer characteristics with those of Vajravelu and Roper[11] and Pal and Hiremath[13] in the presence of internal heat generation/absorption is shown in Table 2. From Tables 1 and 2, one can notice that there is a close agreement with these approaches, which verifies the accuracy of the present method.

Table 2 Comparison of heat transfer characteristics at wall $\theta'(0)$ for $\beta = \alpha = M = f_0 = 0$ and $\delta = -1$

Pr	Vajravelu and Roper[11]		Pal and Hiremath[13]		Present result	
	Ec=0.00	Ec=0.02	Ec=0.00	Ec=0.02	Ec=0.00	Ec=0.02
1	−1.710 937	−1.705 156	−1.710 937	−1.705 156	−1.710 936	−1.705 154
2	−2.486 000	−2.476 280	−2.485 999	−2.476 278	−2.485 998	−2.476 278
3	−3.082 179	−3.069 193	−3.082 174	−3.069 188	−3.082 178	−3.069 192
4	−3.585 194	−3.569 342	−3.585 191	−3.569 339	−3.585 193	−3.569 341
5	−4.028 535	−4.010 094	−4.028 530	−4.010 089	−4.028 536	−4.010 095

The dimensionless velocity profiles for the fluid and the dust phase for different values of the magnetic parameter M with the constant suction parameter are presented in Fig. 1. It is clearly observed that the horizontal velocity profiles decrease with the increases in η and the magnetic parameter. Furthermore, it shows that the momentum boundary layer thickness decreases as M increases and hence induces an increase in the absolute value of the velocity gradient at the surface. The effect of the unsteadiness parameter α on the velocity distribution for both the fluid and the dust phases as a function of η is shown in Fig. 2. It is interesting to note that the velocity profiles decrease with the increase in the value of the unsteadiness parameter.

Figure 3 is plotted for the velocity profiles for different values of the local fluid-particle interaction parameter β. It is found that, if β increases, the fluid phase velocity $f'(\eta)$ decreases, whereas the dust phase velocity $F(\eta)$ increases. For large values of β, the relaxation time of

the dust particle decreases. Then, both the velocities of the fluid and the dust particle will be the same.

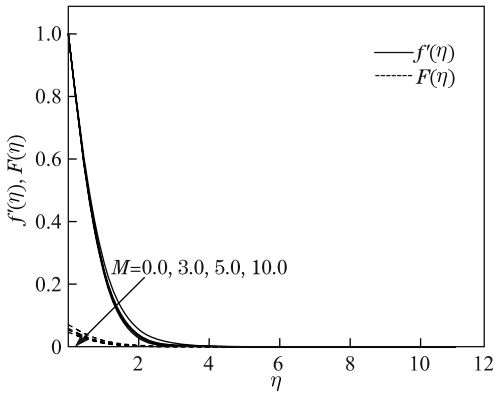

Fig. 1 Effect of magnetic parameter M on velocity profiles

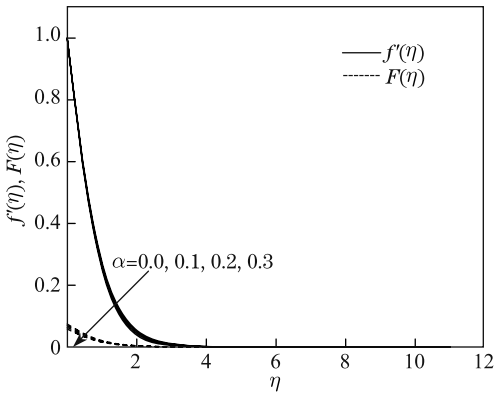

Fig. 2 Effect of variable unsteadiness parameter α on velocity profiles

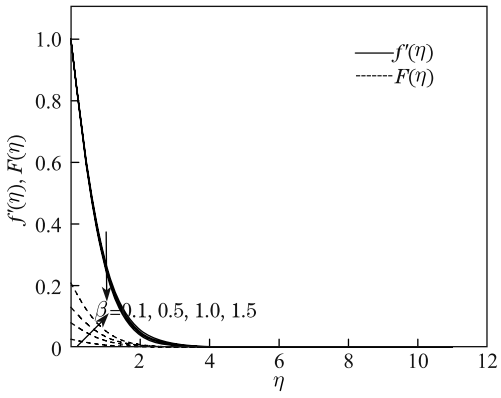

Fig. 3 Effect of local fluid interaction parameter β on velocity profiles

Figures 4(a) and 4(b) represent the temperature profiles for different values of the unsteadiness parameter α for the VWT and VHF cases, respectively. One can observe from these figures that the temperature profiles decrease smoothly with an increase in the unsteadiness parameter α. This shows an important fact that the rate of cooling is much faster for higher values of the unsteadiness parameter, whereas it may take longer time in the steady flow.

Figures 5(a) and 5(b) are the graphical representations of the temperature profiles for different values of the local fluid-particle interaction parameter β. From these figures, it is noted that the temperature distributions of the fluid and the dust phase decrease with an increase in the fluid-particle interaction parameter.

The effect of the Prandtl number Pr on the temperature profiles is shown in Figs. 6(a) and 6(b) for the cases of VWT and VHF, respectively. It is evident from these plots that the temperature distribution continuously decreases within the boundary layer for all values of Pr. This is consistent with the well-known fact that the thermal boundary layer thickness decreases drastically for high values of Pr. Moreover, it shows that the rate of cooling is faster in the case of higher Prandtl numbers.

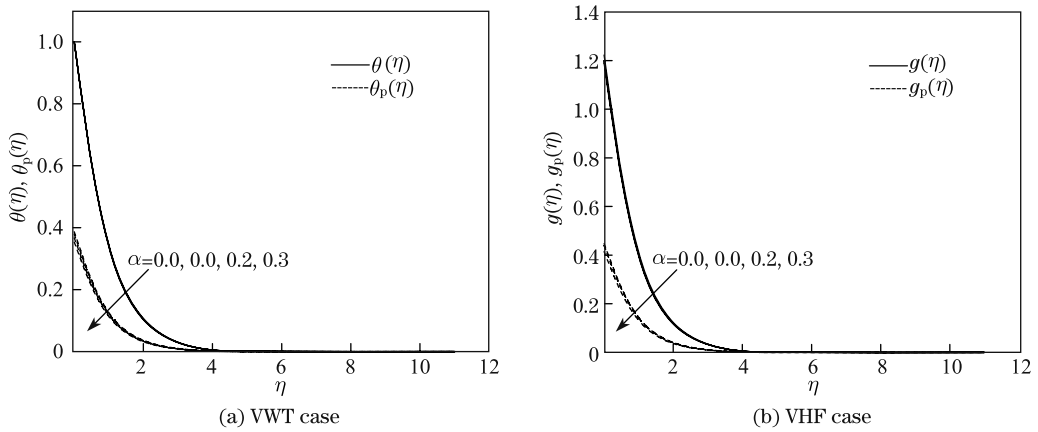

(a) VWT case (b) VHF case

Fig. 4 Effect of unsteadiness parameter α on temperature distributions with $Pr = 0.72, Ec = 2.0, N = 0.5, \delta = 0.1, f_0 = 2.0, \beta = 0.4$, and $E = 2.0$

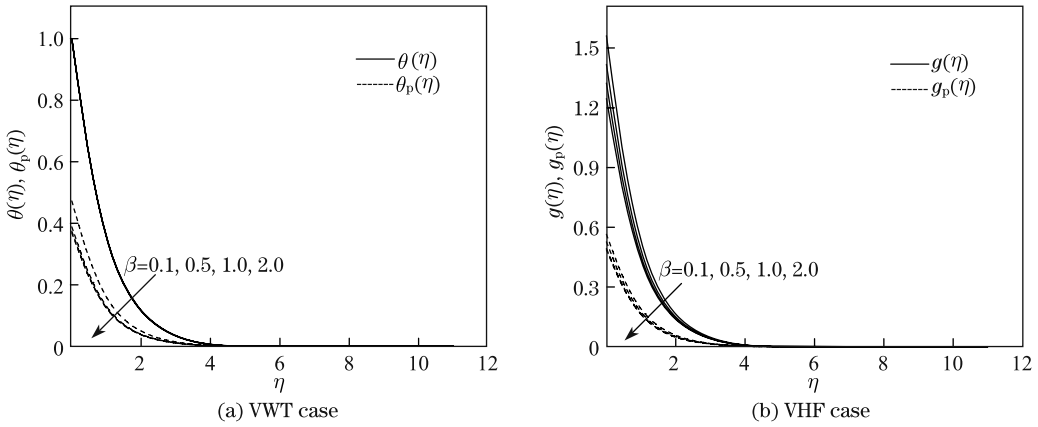

(a) VWT case (b) VHF case

Fig. 5 Effect of local fluid interaction parameter β on temperature distributions with $Pr = 0.72, Ec = 2.0, N = 0.5, \delta = 0.1, f_0 = 2.0, \alpha = 0.2$, and $E = 2.0$

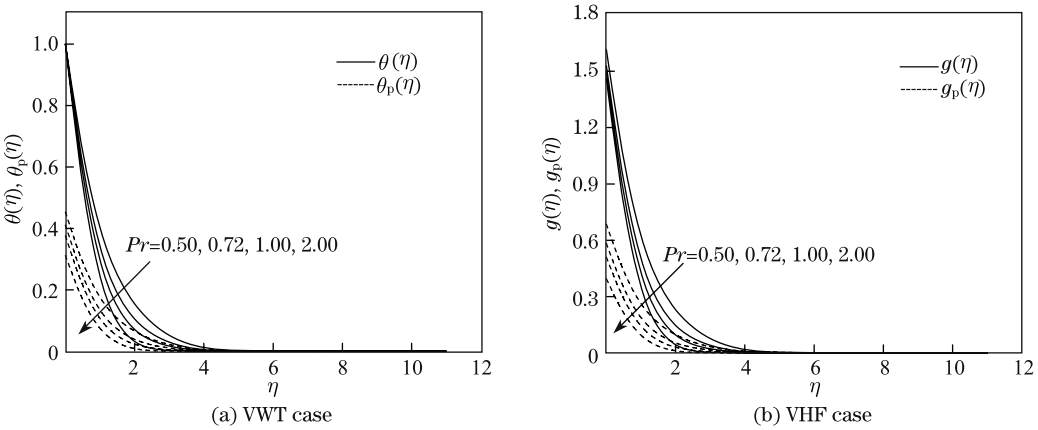

(a) VWT case (b) VHF case

Fig. 6 Effect of Prandtl number Pr on temperature distributions with $Ec = 2.0, N = 0.5, \alpha = 0.2, \delta = 0.1, f_0 = 2.0, \beta = 0.4$, and $E = 2.0$

The graphs for the temperature distribution from the sheet for different values of the Eckert number are plotted in Figs. 7(a) and 7(b) for the VWT and VHF cases. The analysis of the graphs reveals the fact that the effect of the increasing values of the Eckert number is to increase the temperature distribution in the flow region in both the VWT and VHF cases. This is due to the fact that the heat energy is stored in liquid with the frictional heating. Also, one can notice that the combined effect of the suction parameter V_w and the increasing values of Eckert number Ec is to reduce the temperature distribution significantly.

Figures 8(a) and 8(b) depict the dimensionless temperature profiles versus η for different values of the number density N for the VWT and VHF cases. Here, we observe that the temperature profiles for both the fluid and the dust particles decrease with an increase in the number density.

Figures 9(a) and 9(b) give the variation of temperature distribution within the boundary layer for various values of the heat source/sink parameter δ for the VWT and VHF cases. It is noted that the temperature distribution increases with an increase in the heat generation parameter, whereas this trend is reverse during heat absorption.

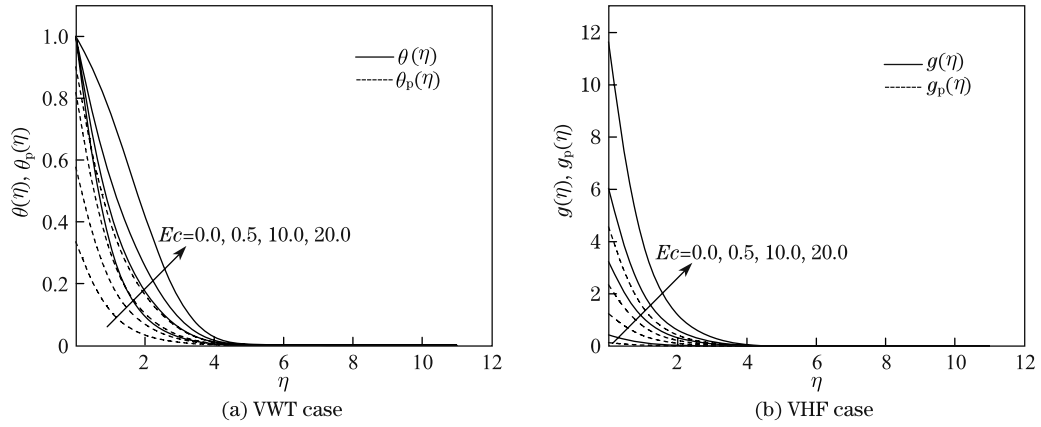

Fig. 7 Effect of Eckert number Ec on temperature distributions with $Pr = 0.72, N = 0.5, \alpha = 0.2, \delta = 0.1, f_0 = 2.0, \beta = 0.4$, and $E = 2.0$

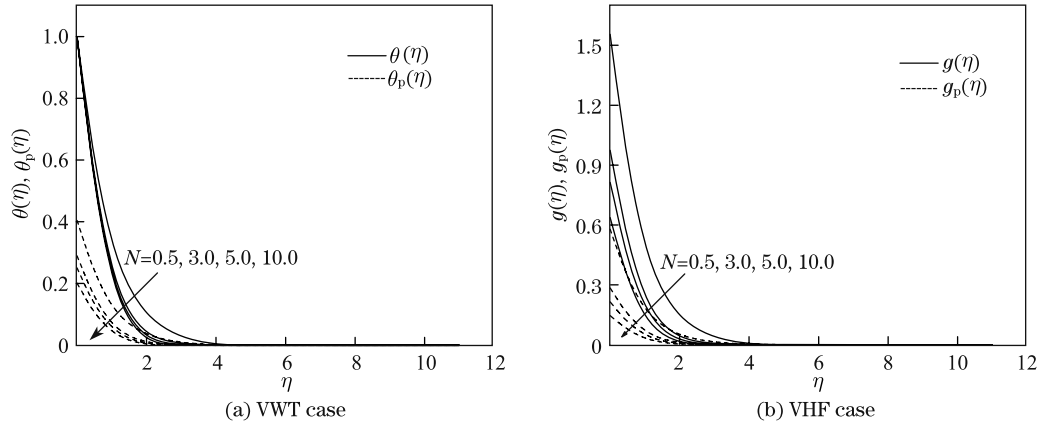

Fig. 8 Effect of number density N on temperature distributions with $Pr = 0.72, Ec = 2.0, \alpha = 0.2, \delta = 0.1, f_0 = 2.0, \beta = 0.4$, and $E = 2.0$

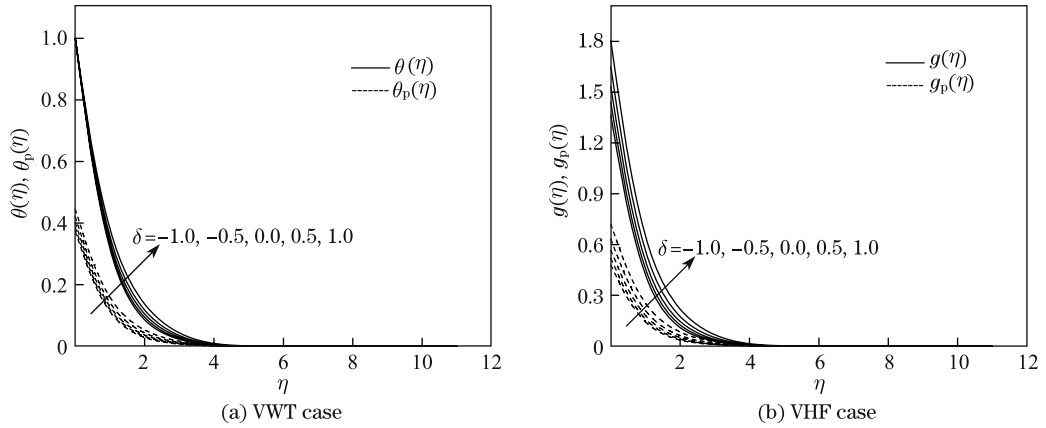

(a) VWT case (b) VHF case

Fig. 9 Effect of source sink parameter δ on temperature distributions with $Pr = 0.72, Ec = 2.0, \alpha = 0.2, N = 0.5, f_0 = 2.0, \beta = 0.4$, and $E = 2.0$

The effects of all the physical parameters on the skin friction coefficient $f''(0)$, the wall temperature gradient $\theta'(0)$, and the temperature function $1/g(0)$ are analyzed in Table 3. It is interesting to note that the effect of the magnetic parameter is to decrease the skin friction coefficient due to the internal absorption parameter ($\delta < 0$). From this table, it is also observed that the surface gradient $f''(0)$ decreases with an increase in the unsteadiness parameter, while the rate of heat transfer increases with the unsteadiness parameter. Furthermore, it is noticed that the effect of the magnetic parameter is to decrease the surface gradient and the rate of heat transfer coefficients.

Table 3 Results of skin friction coefficient and heat transfer characteristics at wall for $Pr = 1.0, Ec = 0.1, \delta = -1, \beta = 0.4$, and $f_0 = 2$

M	α	$f''(0)$	$-\theta'(0)$	$1/g(0)$
	0.1	−2.700 252	2.891 061	2.510 319
0.0	0.2	−2.743 656	2.927 758	2.543 303
	0.3	−2.786 456	2.964 381	2.576 135
	0.1	−2.842 553	2.879 824	2.498 960
0.5	0.2	−2.883 168	2.916 705	2.531 699
	0.3	−2.923 237	2.953 541	2.564 333
	0.1	−2.974 439	2.869 388	2.488 059
1.0	0.2	−3.012 761	2.906 439	2.520 608
	0.3	−3.050 583	2.943 466	2.553 086
	0.1	−3.214 448	2.850 395	2.467 484
2.0	0.2	−3.249 187	2.887 750	2.499 753
	0.3	−3.283 494	2.925 110	2.531 999

Variations of the skin friction coefficient $f''(0)$ with M for different values of β and α are presented in Figs. 10 and 11, respectively. From these graphs, one can notice that the effect of the magnetic parameter is to decrease the skin friction coefficient. Furthermore, it is also observed that $f''(0)$ decreases with the increases in the local fluid-interaction parameter and the unsteadiness parameter.

Figure 12 illustrates the variation of the heat transfer characteristics with the magnetic parameter for various values of the Prandtl number. It is seen from this figure that the rate of heat transfer increases with an increase in the magnetic parameter. It is also evident that

$\theta'(0)$ is negative, and $g(0)$ is positive for all values of the magnetic parameter and the Prandtl number. Moreover, it is observed that there is an increase in the rate of heat transfer as the Prandtl number increases, and also it is clear from Table 3.

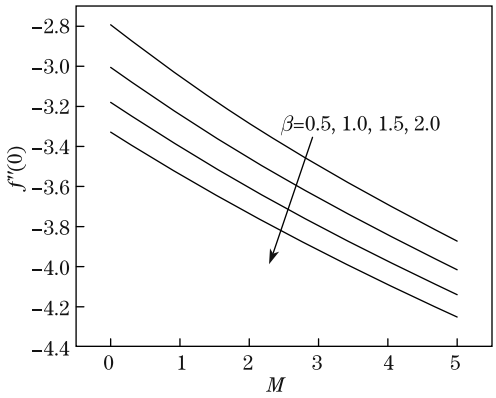

Fig. 10 Skin friction coefficient for various values of β

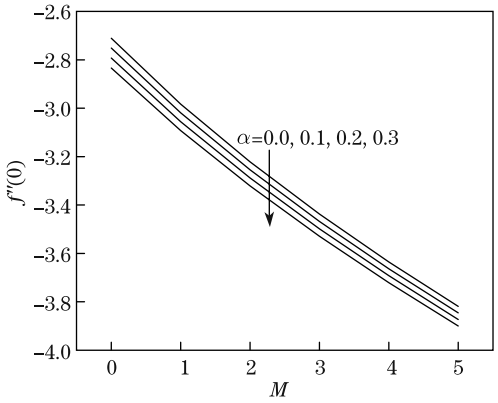

Fig. 11 Skin friction coefficient for various values of α

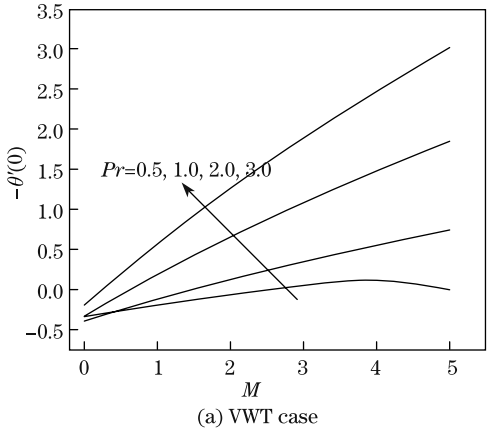

(a) VWT case

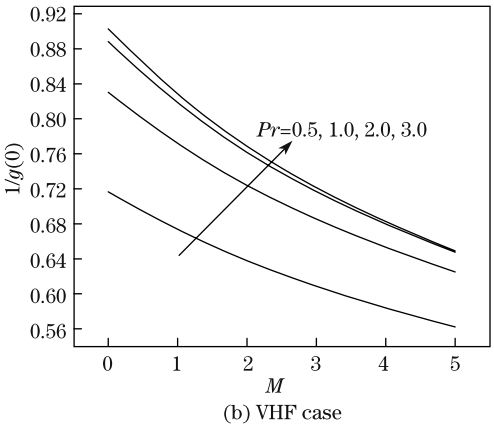

(b) VHF case

Fig. 12 Heat transfer characteristics at wall for different values of Prandtl number Pr

6 Conclusions

An analysis is carried out to study the boundary layer flow and heat transfer of a dusty fluid over an unsteady stretching surface in the presence of non-uniform heat source/sink. Viscous dissipation is included in the energy equation. The basic equations governing the flow are in the form of highly non-linear partial differential equations. These equations are converted into a set of non-linear ordinary differential equations using similarity transformations. The coupled ordinary differential equations are numerically solved by the Runge-Kutta-Fehlberg-45 method using the software MAPLE. The effects of the magnetic parameter, the local fluid-particle interaction parameter, the number density of the dust particles, the Prandtl number, the Eckert number, the heat source/sink parameter, and the unsteadiness parameter on the dynamics are graphically presented. The values of thermal heat characteristics at the wall temperature gradient functions $\theta'(0)$ and $\theta_{\rm p}(0)$ (the VWT case) and wall temperatures $g(0)$ and $g_{\rm p}(0)$ (the VHF case) are tabulated in Table 4. The important conclusions are summarized as follows.

Table 4 Values of wall temperature gradient (for VWT case) and wall temperature (for VHF case)

α	β	N	Pr	Ec	δ	VWT case		VHF case	
						$\theta'(0)$	$\theta_{\rm p}(0)$	$g(0)$	$g_{\rm p}(0)$
0.0	0.1	0.2	0.72	2.0	0.5	−0.364 904	0.357 540	1.276 119	0.433 473
0.1	0.1	0.2	0.72	2.0	0.5	−0.386 949	0.366 779	1.262 878	0.441 483
0.2	0.1	0.2	0.72	2.0	0.5	−0.408 099	0.374 163	1.250 384	0.447 310
0.2	0.0	0.2	0.72	2.0	0.5	−0.600 051	0.614 374	1.175 804	0.704 931
0.2	0.2	0.2	0.72	2.0	0.5	−0.549 913	0.414 201	1.191 115	0.476 944
0.2	0.4	0.2	0.72	2.0	0.5	−0.454 623	0.381 732	1.230 778	0.450 770
0.2	0.1	0.5	0.72	2.0	0.5	−0.408 099	0.374 163	1.250 384	0.447 310
0.2	0.1	1.0	0.72	2.0	0.5	−0.724 629	0.341 228	1.102 440	0.368 515
0.2	0.1	2.0	0.72	2.0	0.5	−1.221 764	0.299 354	0.931 253	0.283 348
0.2	0.1	0.2	0.50	2.0	0.5	−0.384 453	0.420 851	1.348 171	0.543 155
0.2	0.1	0.2	0.72	2.0	0.5	−0.408 099	0.374 163	1.250 384	0.447 310
0.2	0.1	0.2	1.00	2.0	0.5	−0.408 180	0.335 845	1.192 329	0.382 522
0.2	0.1	0.2	0.72	0.0	0.5	−2.363 966	0.292 138	0.423 017	0.123 579
0.2	0.1	0.2	0.72	1.0	0.5	−1.386 033	0.333 150	0.836 701	0.285 444
0.2	0.1	0.2	0.72	2.0	0.5	−0.408 099	0.374 163	1.250 384	0.447 310
0.2	0.1	0.2	0.72	2.0	−0.5	−0.595 325	0.356 728	1.161 414	0.401 928
0.2	0.1	0.2	0.72	2.0	0.0	−0.440 969	0.370 988	1.234 006	0.438 835
0.2	0.1	0.2	0.72	2.0	0.5	−0.268 249	0.388 261	1.324 027	0.486 078

(i) The thickness of the momentum boundary layer decreases with the increases in the magnetic parameter and the unsteadiness parameter in both the fluid and the particle velocity.

(ii) The velocity of the fluid phase decreases with an increase in the fluid-interaction parameter, while the velocity of the dust phase increases with the increasing value of β.

(iii) In both the VWT and VHF cases, the temperature decreases with the increases in the unsteadiness parameter and the fluid-particle interaction parameter.

(iv) The Prandtl number reduces both the temperature distribution and the heat transfer rate for its increasing values.

(v) The temperature profile decreases with an increase in the value of the number density, while it increases with the increases in the Eckert number and the heat source/sink parameter. The flow of heat becomes faster when Ec increases.

(vi) The surface gradient is negative and decreases with the increases in the unsteadiness parameter and the magnetic parameter.

(vii) The local Nusselt number increases with an increase in the unsteadiness parameter for both the VWT and VHF cases, whereas the reverse trend is seen with an increase in the magnetic parameter.

Acknowledgements The authors wish to express their sincere thanks to the referees for their valuable comments and suggestions.

References

[1] Sakiadis, B. C. Boundary layer behavior on continuous solid surfaces: I. boundary layer equations for two dimensional and axisymmetric flow. *AIChE Journal*, **7**(1), 26–28 (1961)

[2] Sakiadis, B. C. Boundary layer behavior on continuous solid surfaces: II. boundary layer behavior on continuous flat surface. *AIChE Journal*, **7**(2), 221–225 (1961)

[3] Crane, L. J. Flow past a stretching plate. *Zeitschrift für Angewandte Mathematik und Physik* (*ZAMP*), **21**(4), 645–647 (1970)

[4] Grubka, L. J. and Bobba, K. M. Heat transfer characteristics of a continuous stretching surface with variable temperature. *Journal of Heat Transfer*, **107**(1), 248–250 (1985)

[5] Chen, C. H. Laminar mixed convection adjacent to vertical, continuously stretching sheets. *Heat and Mass Transfer*, **33**(5-6), 471–476 (1998)

[6] Elbashbeshy, E. M. A. and Bazid, M. A. A. Heat transfer over an unsteady stretching surface. *Heat and Mass Transfer*, **41**(1), 1–4 (2004)

[7] Sharidan, S., Mahmood, T., and Pop, I. Similarity solutions for the unsteady boundary layer flow and heat transfer due to a stretching sheet. *International Journal of Applied Mechanics and Engineering*, **11**(3), 647–654 (2006)

[8] Tsai, R., Huang, K. H., and Huang, J. S. Flow and heat transfer over an unsteady stretching surface with a non-uniform heat source. *International Communications in Heat and Mass Transfer*, **35**(10), 1340–1343 (2008)

[9] Ishak, A., Nazar, R., and Pop, I. Hydromagnetic flow and heat transfer adjacent to a stretching vertical sheet. *Heat and Mass Transfer*, **44**(8), 921–927 (2008)

[10] Aziz, A. A similarity solution for laminar thermal boundary layer over a flat plate with a convective surface boundary condition. *Communications in Nonlinear Science and Numerical Simulation*, **14**(4), 1064–1068 (2009)

[11] Vajravelu, K. and Roper, T. Flow and heat transfer in a second grade fluid over a stretching sheet. *International Journal of Non-Linear Mechanics*, **34**(6), 1031–1036 (1999)

[12] Chen, C. H. Combined heat and mass transfer in MHD free convection from a vertical surface with Ohmic heating and viscous dissipation. *International Journal of Engineering Science*, **42**(7), 699–713 (2004)

[13] Pal, D. and Hiremath, P. S. Computational modelling of heat transfer over an unsteady stretching surface embedded in a porous medium. *Meccanica*, **45**(3), 415–424 (2010)

[14] Vajravelu, K. and Hadjinicolaou, A. Heat transfer in a viscous fluid over a stretching sheet with viscous dissipation and internal heat generation. *International Communications in Heat and Mass Transfer*, **20**(3), 417–430 (1993)

[15] Veena, P. H., Subhas-Abel, M., Rajagopal, K., and Pravin, V. K. Heat transfer in a visco-elastic fluid past a stretching sheet with viscous dissipation and internal heat generation. *Zeitschrift für Angewandte Mathematik und Physik* (*ZAMP*), **57**(3), 447–463 (2006)

[16] Saffman, P. G. On the stability of laminar flow of a dusty gas. *Journal of Fluid Mechanics*, **13**, 120–128 (1962)

[17] Datta, N. and Mishra, S. K. Boundary layer flow of a dusty fluid over a semi-infinite flat plate. *Acta Mechanica*, **42**, 71–83 (1982)

[18] Agranat, V. M. Effect of pressure gradient on friction and heat transfer in a dusty boundary layer. *Fluid Dynamics*, **23**, 729–732 (1988)

[19] Vajravelu, K. and Nayfeh, J. Hydromagnetic flow of a dusty fluid over a stretching sheet. *International Journal of Non-Linear Mechanics*, **27**(6), 937–945 (1992)

[20] Xie, M. L., Lin, J. Z., and Xing, F. T. On the hydrodynamic stability of a particle-laden flow in growing flat plate boundary layer. *Journal of Zhejiang University SCIENCE A*, **8**, 275–284 (2007)

[21] Palani, G. and Ganesan, P. Heat transfer effects on dusty gas flow past a semi-infinite inclined plate. *Forsch Ingenieurwes*, **71**, 223–230 (2007)

[22] Gireesha, B. J., Ramesh, G. K., Subhas-Abel, M., and Bagewadi, C. S. Boundary layer flow and heat transfer of a dusty fluid flow over a stretching sheet with non-uniform heat source/sink. *International Journal of Multiphase Flow*, **37**(8), 977–982 (2011)

[23] Schlichting, H. *Boundary Layer Theory*, McGraw-Hill, New York (1968)